Journal of Catalysis **192,** 381–390 (2000)
doi:10.1006/jcat.2000.2858, available online at http://www.idealibrary.com on IDEAL®

Dissociative Adsorption of N_2 on Ru(0001): A Surface Reaction Totally Dominated by Steps

S. Dahl,* E. Törnqvist,† and I. Chorkendorff*,‡

*Center for Atomic-Scale Materials Physics (CAMP), Department of Physics, Technical University of Denmark, DK-2800 Lyngby, Denmark; †Haldor Topsøe Research Laboratories, DK-2800 Lyngby, Denmark; and ‡Interdisciplinary Research Center for Catalysis (ICAT), Technical University of Denmark, DK-2800 Lyngby, Denmark
E-mail: sordahl@fysik.dtu.dk

Received November 1, 1999; revised February 15, 2000; accepted February 16, 2000

The dissociative chemisorption of N_2 on Ru(0001) was studied by thermal adsorption. On the clean Ru(0001) surface the initial sticking coefficient was determined to be $s_0 = 10^{-5.4 \pm 0.7} \times \exp(-36 \pm 5\,\mathrm{kJ\,mol^{-1}\,R^{-1}\,T^{-1}})$. With the deposition of less than 0.01 monolayer of Au on the Ru(0001) surface the initial sticking coefficient of N_2 dramatically decreased to $s_0 = 10^{-3.5 \pm 1.7} \times \exp(-126 \pm 21\,\mathrm{kJ\,mol^{-1}\,R^{-1}\,T^{-1}})$, which corresponds to seven orders of magnitude at 500 K. Since Au preferentially adsorbs at the steps on the Ru(0001) surface we conclude that N_2 dissociation is exclusively taking place at the few step sites on the clean Ru(0001) surface. The desorption of N_2 from the Ru(0001) surface was also strongly affected by the presence of small amounts of Au; the TPD peak was shifted up by roughly 150 K. By simulating the TPD spectra we find that this shift corresponds to a difference in the desorption barrier of about 73 kJ/mol for desorption from the steps and from the terraces. The implications of the results for Ru as an ammonia synthesis catalyst are discussed.

1. INTRODUCTION

Promoted Ru catalysts are highly active for ammonia synthesis and have been suggested as alternatives to the traditional Fe catalysts (1). It is well established that dissociative chemisorption of N_2 is the rate-determining step in ammonia synthesis over Fe catalysts. Gaining insight into the N_2 dissociation reaction over Ru is therefore important in the course of reaching a microscopic understanding of ammonia synthesis over Ru. Consequently there has recently been great interest in studying N_2 adsorption on Ru surfaces and catalysts. Measurements of the N_2 dissociation rate over Ru catalysts resulted in an activation energy barrier between 27 and 60 kJ/mol for the process (2, 3), which is in fair agreement with a dissociation probability for nitrogen of 10^{-12} at 300 K measured over three different Ru surfaces (4); a review of these results is given by Jacobi (5). Time-of-flight thermal desorption measurements show N_2 molecules desorbing from Ru(0001) to have average kinetic energies of about 63 kJ/mol, confirming a barrier for adsorption of this order of magnitude (6). Contrary to this, density functional calculations have shown a dissociation barrier of 131 kJ/mol on the Ru(0001) surface (7), and more recent calculations using a more accurate exchange-correlation description result in an even higher barrier (6). Supersonic molecular beam experiments indicate a barrier of 100–200 kJ/mol for the dissociation process (8). Ammonia synthesis over a stepped Ru(0001) single crystal resulted in an apparent activation energy of 101 kJ/mol for the reaction (9), close to values obtained over supported Ru catalysts (10). If N_2 dissociation is rate determining, this implies an activation energy lower than 101 kJ/mol for this process, since part of the apparent activation energy for the ammonia synthesis reaction comes from the energy cost of creating free sites on the surface (11).

The desorption of N_2 from the Ru(0001) surface has been reported after preparation of chemisorbed N atoms by either decomposition of NH_3 or adsorption of excited N_2 molecules, and in the low N coverage regime the desorption barrier was found to be 184–190 kJ/mol (12, 13).

Metal surfaces are not perfectly flat; there will always be a small concentration of atomic steps. It has long been realized that steps at metal surfaces may provide sites with higher reactivity than terrace sites. The concept of special "active sites" associated with low-coordinated surface atoms was introduced as early as in 1925 by Taylor (14). In support of this, studies of high-index surfaces have shown that steps are special and important in many surface chemical reactions (15–17); e.g., it was seen that CO only dissociates at the steps of an Ru(0001) surface (17). Most recently, it was directly observed using scanning tunneling microscopy (STM) that NO preferentially dissociates at steps on an Ru(0001) surface (18). Therefore a possible way of reconciling the different experiments and calculations for N_2 dissociation on Ru is to propose that the thermal experiments are in fact not probing the dissociation process on the terrace sites but are measuring the rate at the few step sites on the single-crystal surface.

0021-9517/00 $35.00

Here we report on rate measurements of N_2 dissociation and associative N_2 desorption at the close-packed Ru(0001) surface and at the steps on this surface. Some of the results in this paper have been published in a letter together with theoretical calculations (19).

Our ultrahigh vacuum (UHV) chamber is equipped with a high-pressure cell enabling exposures of large doses of N_2 within a relatively short time and at elevated temperatures. This is important since the sticking coefficient is very low, and it also ensures that the reacting gas is equilibrated with the surface. On the clean Ru(0001) surface the initial sticking coefficient was determined to be $s_0 = 10^{-5.4 \pm 0.7} \times \exp(-36 \pm 5 \text{ kJ mol}^{-1} \text{R}^{-1} \text{T}^{-1})$.

To investigate if steps are controlling a surface reaction, one generally compares the reactivity of low-index surfaces with the reactivity of high-index surfaces which have higher step densities (15–17). This approach will only show a reactivity difference corresponding to the difference in step concentration on the two surfaces (up to two orders of magnitude), and the reactivity of the flat terrace is inaccessible. However, it can be possible to measure both the reactivity of the steps and the terraces if the steps are strongly poisoned by the adsorbates originating from the dissociation process (20). We use a different approach to investigate if the reactivity of the clean Ru(0001) surface is dominated by step sites. STM work by Behm and co-workers on the Au/Ru(0001) system has shown that Au will preferentially decorate the steps on the surface (21). Therefore, given the nobleness of Au, small amounts of Au on the Ru(0001) surface are expected to suppress the reactivity of the few steps present and make it possible to determine the importance of steps for N_2 dissociation. In this way, it should also be possible to measure the reactivity of both the steps and the flat terraces. Indeed, the deposition of less than 0.01 monolayer of Au on the Ru(0001) surface had a dramatic effect, decreasing the initial sticking coefficient of N_2 to at least $s_0 = 10^{-3.5 \pm 1.7} \times \exp(-126 \pm 21 \text{ kJ mol}^{-1} \text{R}^{-1} \text{T}^{-1})$, or seven orders of magnitude at 500 K compared to the clean surface. Therefore we conclude that N_2 dissociation is exclusively taking place at the few step sites on the clean Ru(0001) surface. Taking into account that the steps only represent about 1% of the surface sites, the difference between the sticking coefficient of the steps and the terraces is nine orders of magnitude.

The associative desorption of nitrogen from the Ru(0001) surface is also strongly affected by the presence of small amounts of Au, resulting in a 150 K upward shift of the N_2 desorption temperature. An obvious explanation would be that desorption from the clean surface is dominated by the steps where the desorption barrier is lower than on the terraces. On the Au-passivated surface this channel is blocked and the desorption process has to take place via the high barrier present at the terrace. Simulation of the TPD spectra using this assumption and a barrier of 145 kJ/mol for desorption at the step and 218 kJ/mol at the terrace agrees well with the experimental observations.

2. EXPERIMENTAL

The experiments were performed in an UHV apparatus with a base pressure of 1×10^{-10} mbar. The setup, which has been described previously (9) is, apart from standard surface science tools, equipped with a high-pressure cell (HPC) where the sample can be exposed to gas pressures up to 10 bar at elevated temperatures without ruining the vacuum in the UHV chamber.

The exposures were done with N_2 at pressures between 0.03 and 3.5 bar, and at surface temperatures between 300 and 700 K. At these pressures, the temperature of the gas molecules close to the surface is almost equal to the surface temperature. In a similar study, it has been shown that 0.1 bar is sufficient to achieve thermal equilibrium between a surface and H_2 molecules (22). H_2 is more difficult to equilibrate than N_2 due to the higher vibration frequency of H_2. We saw no systematic differences between the sticking coefficients measured using a pressure of 0.03 bar and those measured using a pressure of 0.1 bar; hence 0.03 bar is apparently a sufficient pressure for achieving thermal equilibrium between the sample surface and N_2.

When the exposures were done at 0.03 or 0.1 bar the filling and evacuation of the high pressure cell was achieved within less than 1 s. At this pressure the filling was done by expanding known volumes of N_2 at 1.5 bar into the high-pressure cell, and the evacuation was done by dumping the gas into a turbo molecular pump. In this manner it was possible to use exposure times down to 10 s. At the higher pressures the filling and evacuation times were 1 min or more, and the exposure times were always at least 10 min. There was no flow of N_2 through the HPC during an experiment. However, for dosing times exceeding 1 h it was necessary to continously supply N_2 to maintain the pressure in the HPC. This was due to gas drainage from the HPC, mainly through the orifice to the mass spectrometer and through a leaky valve. The N_2 used (Nitrogen N60, Air Liquide) had less than 1 ppm of impurities as received, and was further purified by being passed over a dry molecular sieve and a freshly reduced Ni catalyst exposing about 10 m^2 of metallic Ni, both at room temperature. This resulted in a gas in which no evidence of impurities was seen, except for hydrogen. After having carried out a few adsorption experiments, we estimated the level of H_2 to approximately 0.2 ppm. This concentration was not constant in all the experiments since some of the H_2 originated from the walls of HPC which had been exposed to high pressures of H_2 in earlier experiments.

CO contamination of the Ru(0001) surface was observed if the sample was kept below 500 K in the UHV chamber.

Therefore, to minimize this the surface was always kept above 500 K in the UHV chamber before it was exposed to N_2 in the HCP.

The Ru(0001) surface used in this study is oriented to within 0.5° of the crystallographic plane, as checked by Laue X-ray diffraction, and therefore has an average step density of 1% or less. The crystal was mounted on tungsten wires going through holes in the crystal that were spark cut parallel to the surface. The wires and the crystal were heated resistively. The crystal temperature was measured by a chromel/alumel thermocouple spotwelded to the edge of the crystal. Cleaning of the surface was achieved by Ar^+ sputtering and by heating the crystal to 1473 K in 2×10^{-8} mbar O_2, and finally annealing at 1473 K for 3 min to desorb oxygen. The cleanliness was verified by X-ray photoelectron spectroscopy (XPS), ion scattering spectroscopy (ISS), and monitoring the desorpotion of CO and CO_2 while heating the crystal in oxygen. The latter was carried out to check for carbon contamination. The N coverage was measured by XPS and by integration of temperature-programmed desorption (TPD) spectra, and the absolute coverage was calibrated against the CO saturation coverage of 0.56 monolayer (ML) at 300 K on Ru(0001) (4).

Gold was deposited on the surface by evaporation of 99.99% pure Au placed in a tungsten cup which was heated by electron bombardment. During deposition the crystal was held at 700 K, which was the highest temperature used when adsorbing N_2 on the Au/Ru(0001) surface. The high diffusivity at this temperature maximizes the possibility of Au ending up at a step rather than forming islands on the wide terraces. The latter was observed at room temperature deposition (21). In addition, using a temperature of 700 K avoids CO contamination of the surface during the deposition. The Au coverage was calibrated by ISS, as seen in Fig. 1, and a correlation between the ISS and XPS signals was established. By performing ISS at different positions on the surface, it was verified that the Au was distributed evenly over the whole surface on a macroscopic scale. After N_2 adsorption on the Au/Ru(0001) surface, the Au coverage was determined by XPS. ISS cannot be used since the adsorbed N will change the Au/Ru ISS peak ratio, which is used to determine the Au coverage.

A differentially pumped quadrupole mass spectrometer (QMS) was employed in the TPD experiments, and a heating rate of 4 K/s was used. Since CO is adsorbed from the UHV background if the sample temperature is below 500 K, we used the signal at $m/z = 14$ amu as a measure of N_2 desorption. It should be noted that the intensity of doubly ionized CO is less than 1% of CO's intensity at 28 amu, while the intensity of N^+ is about 14% of the signal from N_2 at 28 amu. In order to only detect molecules desorbing from the front of the crystal, it was positioned approximately 0.3 mm from a 3-mm hole in the differentially pumped QMS housing. This was, however, not sufficient to totally eliminate contributions from molecules desorbing from other surfaces. This was especially evident in experiments in which the front surface was covered with a full monolayer of Au and the crystal was exposed to very large doses of N_2. In such experiments XPS showed that there was no N adsorbed on the front surface, but subsequent TPD showed an N_2 signal corresponding to up to 0.05 ML of nitrogen on the front surface. This signal originated from N_2 desorbing partly from other surfaces of the crystal where there was no gold adsorbed, and mostly from the W-wires. This was clear from the fact that after an N_2 dose, TPD showed a huge N_2 signal when the tungsten wires were positioned in front of the hole in the QMS housing, which can only be explained by desorption of nitrogen that was dissolved in the bulk of the tungsten wires. It turned out that this "background" signal in the N_2 TPD experiments was proportional to the simultaneous change in the UHV chamber pressure as measured by the ionization gauge. The increase in background pressure due to N_2 desoption from the W-wires was up to 2×10^{-8} mbar. Therefore, it was possible to correct for the "background" by recording the UHV pressure during the N_2 TPD experiments and subtracting a signal proportional to the change in this pressure from the N_2 TPD signal. This was done in all the experiments in which it was of any significance for the results. The correction procedure is illustrated in the inset of Fig. 9.

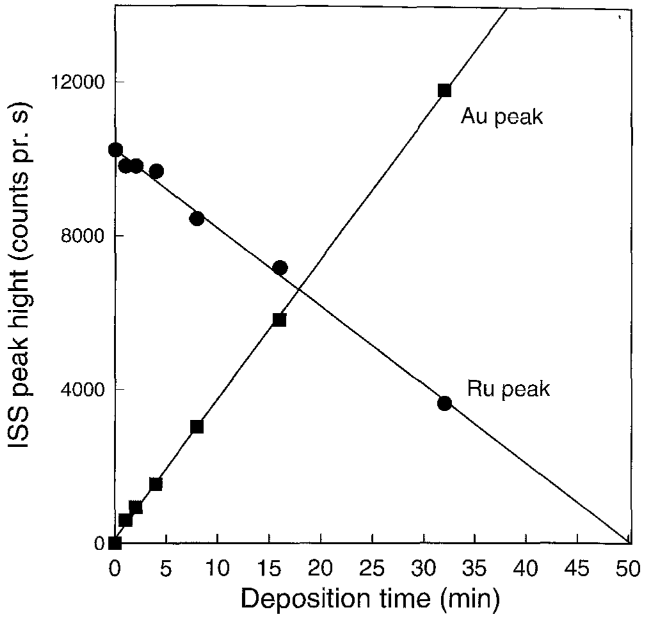

FIG. 1. ISS peak heights of Ru and Au peaks as a function of Au deposition time. ISS is only probing the outermost surface atoms; therefore the amount of Au on the surface after a deposition time of 50 min corresponds to the whole Ru(0001) surface being covered with Au. We define this as 1 ML of gold.

3. RESULTS

The coverages of N on the clean Ru(0001) surface after different dosing conditions are shown in Fig. 2. Second-order Langmuir adsorption kinetics is assumed.

$$\frac{d\Theta}{dt} = 2s_0F\left(1 - \frac{\Theta}{\Theta_{\text{sat}}}\right)^2 \qquad [1]$$

Here, Θ is the coverage and Θ_{sat} the saturation coverage of nitrogen, F is the flux of N_2 in units of monolayer, and the factor of 2 stems from the fact that one adsorbed N_2 molecule will dissociate and occupy two sites on the surface. The flux F can be written as

$$F = \frac{P}{N_{\text{Ru(0001)}}\sqrt{2\pi mk_BT}}, \qquad [2]$$

where P is the N_2 pressure, m is the mass of an N_2 molecule, T is the gas temperature, and $N_{\text{Ru(0001)}}$ is the surface density of Ru atoms in the Ru(0001) surface (1.57×10^{19} m^{-2}).

Integration of Eq. (1) leads to

$$\Theta = \frac{2s_0Ft}{1 + (2s_0Ft/\Theta_{\text{sat}})}, \qquad [3]$$

where t is the exposure time. The data in Fig. 2 is fitted to this expression at each temperature.

Diffusion of N on Ru(0001) is very slow at room temperature; the jump rate is about one jump per minute at 300 K, and the barrier for diffusion is reported to be 91 kJ/mol (23). At temperatures close to room temperature, diffusion will consequently be the limiting factor for N adsorption after some time where the areas close to the steps have been saturated with N. Therefore, the Θ_{sat} used is not the same for all the curves in Fig. 2. At 300 K there is also, apart from N, a significant amount of H adsorbed on the surface, which probably will lower Θ_{sat} since the adsorbed H will block the sites for N adsorption. These complications introduce a large uncertainty in the value of s_0 at 300 K. However, the value is in good agreement with similar measurements by Dietrich *et al.* (4), and in the Arrhenius plot of our data in Fig. 3, their data point is shown as the filled square. The fit of our data to the Arrhenius expression yields $s_0 = 10^{-5.4\pm0.7} \times \exp(-36 \pm 5 \text{ kJ mol}^{-1}\text{R}^{-1}\text{T}^{-1})$.

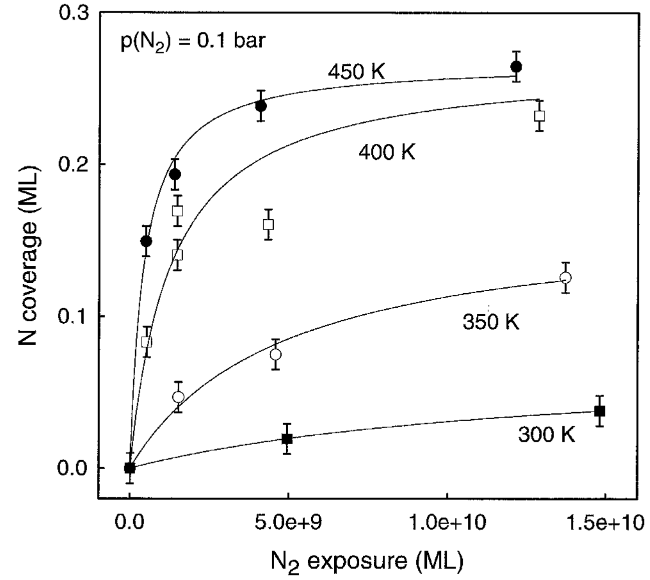

FIG. 2. Coverage of N on a clean Ru(0001) surface as a function N_2 exposure. The N coverage was measured with XPS. The solid lines are best fits assuming second-order adsorption (Eq. [3]), from which the initial sticking coefficients (s_0) were determined.

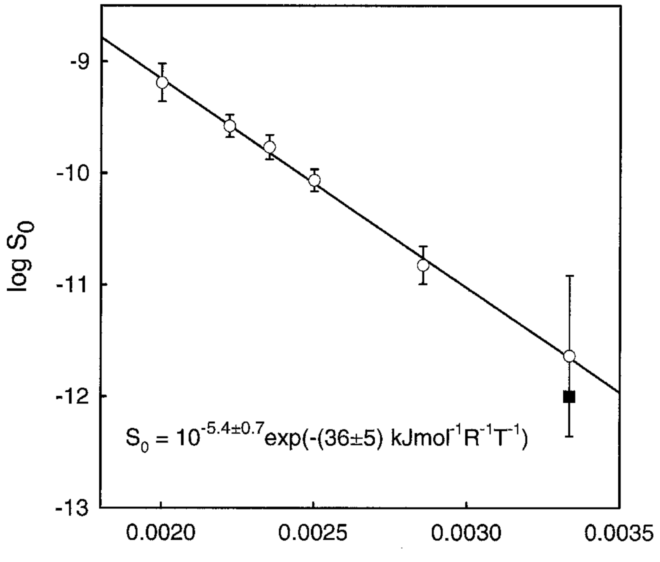

FIG. 3. Arrhenius plot of the initial sticking coefficient of N_2 on the clean Ru(0001) surface. The filled square is the result from a similar experiment at room temperature by Dietrich *et al.* (4).

We now turn to N_2 adsorption on the Au-passivated Ru(0001) surfaces. As pointed out in the introduction, Behm and co-workers have reported that Au will preferentially adsorb at step sites on the Ru(0001) surface (21). This observation was done at room temperature, and it is an open question whether it is also the case at higher temperatures. Behm and co-workers reported that only the shape and not the size of Au islands was changed by annealing the surface at 650 K (21). Their interpretation of this observation was that gold atoms can diffuse along the perimeter of the islands but cannot dissociate from them at 650 K. Therefore, Au will presumably stay at the steps during our N_2 adsorption experiments where $T \leq 700$ K. Figure 4 displays the results of an experiment where the N_2 dosing conditions were kept constant (0.1 bar N_2 at 500 K for 1 min) at different Au coverages of the Ru(0001) surface. As seen in the figure, there is a dramatic drop in the N coverage when less than 0.01 ML of Au is deposited on the surface. The only

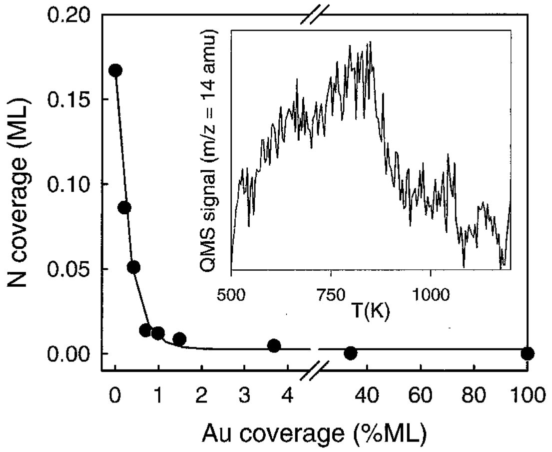

FIG. 4. The N coverage on Ru(0001) after a fixed dose of N_2 (0.1 bar, 1 min, 500 K) as a function of Au coverage on the surface. The nitrogen coverages were determined by integrating the subsequent N_2 TPD spectra ($m/z = 14$ amu). A contribution to the TPD signal, originating from other surfaces, was subtracted as described in the text. The inset shows the N_2 TPD spectrum ($m/z = 14$ amu) used to obtain the coverage on the Ru(0001) surface covered with 0.037 ML of Au. The spectrum was "background" corrected as described in the text.

reasonable interpretation of this is that the N_2 dissociation observed on the clean Ru(0001) surface is dominated by the dissociation at step sites whose abundance is less than 1% of the total number of sites, and which are blocked by Au.

The N coverages in Fig. 4 were measured by integration of the N_2 signal at $m/z = 14$ amu in the TPD experiments following the N_2 dose. For Au coverages in the region 0.01–0.04 ML in Fig. 4, the N coverage does not drop, even after "background" correction, to the low level close to zero expected from the quantitative dissociation rate measurements of Fig. 6. A plausible explanation is that there are regions at the front surface where the step density is still higher than the Au coverage so that N adsorption at steps can still proceed in these limited regions. This is supported by the fact that the "background"-corrected N_2 desorption signal from an Ru(0001) surface covered with 0.037 ML of Au is appearing in the same temperature region as desorption from clean Ru(0001); this is shown in the inset of Fig. 4.

To quantify the difference between the clean and the Au-passivated Ru(0001) surface, the dissociative adsorption of N_2 on the latter surface was also studied. In order to minimize the possibility that Au is affecting sites on the surface other than the step sites, surfaces covered with 0.01–0.02 ML of Au were investigated. The resulting N coverages as a function of N_2 exposure at temperatures between 620 and 700 K are shown in Fig. 5. As for the clean surface the data were fitted to the second-order uptake expression (Eq. [3]) using a zero-point correction of 0.01–0.016 ML of N. As discussed above, this correction is due to the N adsorbed on areas at the Ru(0001) surface where the Au coverage was insufficient to cover all the step sites. The zero-point levels are small and not very important for the results. They were estimated from the measured nitrogen coverage after relatively small doses of N_2 where the N coverage should have been very close to zero if all the step sites on the surface had been blocked.

Experiments carried out at temperatures lower than 620 K resulted in N coverages that were not reproducible, and the data apparently followed first-order adsorption kinetics instead of the second-order kinetics observed at higher temperatures. The adsorption rate also seemed to become independent of temperature. The very low sticking coefficients at these temperatures ($s_0 \leq 10^{-14}$) are at the limit of what is possible to measure, and it is quite possible that the results are influenced by trace amounts of impurities in the gas. Normally, gas impurities below 0.01 ppm will not be a problem since the sample is exposed to such a small amount of gas during an experiment that the adsorption of all impurities would only result in a very small coverage. However, NH_3 is a special case since it could be produced *in situ* from N_2 and the small amounts of H_2 in the gas, on the backside of the crystal where no Au is deposited. The equilibrium mole fraction of ammonia in 2 bar of nitrogen with 0.2 ppm of hydrogen is 7×10^{-12} at 600 K. If the decomposition probability for an ammonia molecule hitting the Au/Ru(0001) surface is about 10^{-3}, this would be sufficient to account for the N coverages observed at temperatures below 620 K. The decomposition probability for ammonia on Ru(0001) is reported by Huang *et al.* to be about 0.03 at 480 K (24), but Dietrich *et al.* find a value closer to 10^{-4} at 500 K (25). H_2 is produced when the

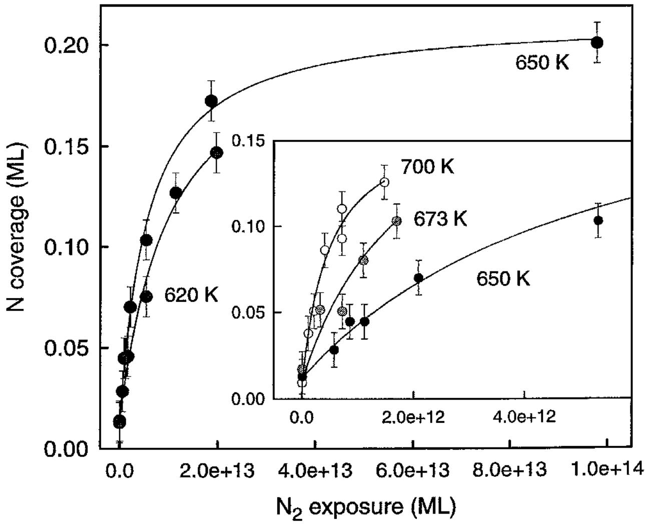

FIG. 5. Coverage of N on an Ru(0001) surface covered with 0.01–0.02 ML of Au as a function of N_2 exposure. The experiments were carried out at N_2 pressures of 0.1 to 3.5 bar, and the exposure time was up to 80 h. The N and Au coverages were measured with XPS. The solid lines are best fits using Eq. [3], from which the initial sticking coefficients (s_0) were determined.

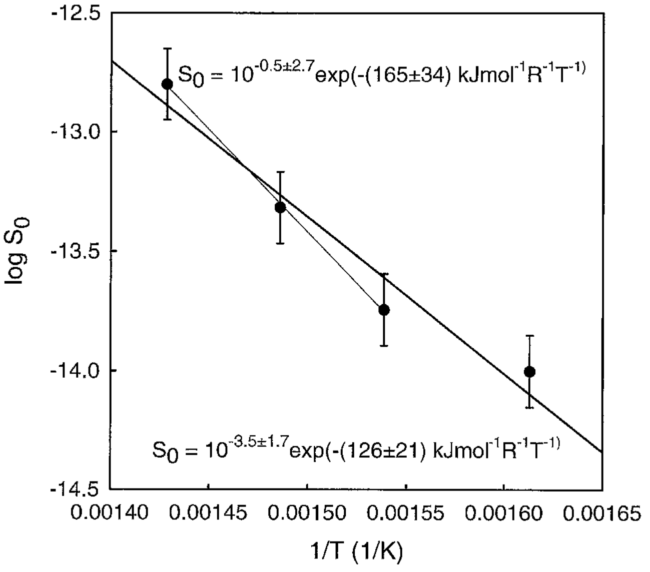

FIG. 6. Arrhenius plot of the initial sticking coefficient of N_2 on the Ru(0001) surface covered with 0.01–0.02 ML Au.

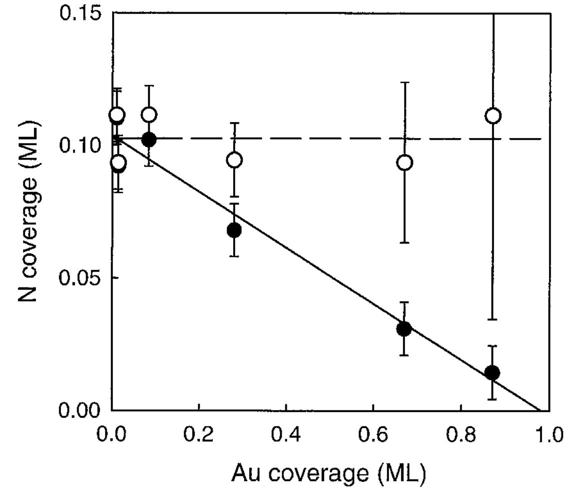

FIG. 7. The N coverage on Ru(0001) after a fixed dose of N_2 (3.5 bar, 40 min, 700 K) as a function of Au coverage on the surface. The filled circles are absolute N coverage measured with XPS, and the open circles are the N coverage relative to the part of the Ru surface not covered by Au.

ammonia decomposes and will therefore not be consumed in the process. A mechanism in which ammonia decomposition is the main source of adsorbed N below 620 K can explain all the observations. The equilibrium concentration of ammonia gets smaller when the temperature is raised, and the direct dissociation of N_2 becomes much faster due to the high activation barrier. N adsorption via ammonia will therefore cease to dominate above a certain temperature (e.g., 620 K), and below this temperature the N adsorption rate could well be independent of temperature. The observed first-order adsorption kinetics is also consistent with N adsorption via NH_3 decomposition. Based on these considerations, we assume that the N adsorption observed at the Au-passivated Ru(0001) surface below 620 K is mainly due to NH_3 decomposition rather than N_2 dissociation. Therefore, measurements below 620 K are not included in the discussion.

The initial sticking coefficients for N_2 adsorption on the Au-passivated Ru(0001) surface are displayed in the Arrhenius plot of Fig. 6. At 620 K, s_0 is high compared to a value obtained by extrapolation from the other data points, which may indicate that the proposed mechanism of N adsorption via ammonia decomposition is already significant at this temperature. Fitting the data results in $s_0 = 10^{-3.5\pm1.7} \times \exp(-126 \pm 21 \text{ kJ mol}^{-1} \text{R}^{-1} \text{T}^{-1})$, and if the data point at 620 K is removed the result is $s_0 = 10^{-0.5\pm2.7} \times \exp(-165 \pm 34 \text{ kJ mol}^{-1} \text{R}^{-1} \text{T}^{-1})$.

To clarify how N_2 adsorption on the Au-passivated Ru(0001) surface depends on the Au coverage, a series of experiments were performed where the Au coverage was varied and the N coverage was measured after a fixed, high N_2 dose (3.5 bar, 40 min, 700 K). The results are displayed in Fig. 7, and it is seen that the N coverage is proportional to the fraction of the Ru(0001) surface which is not covered with Au. This is the expected result if the Au forms islands and/or grows from the steps, and the N_2 dissociation occurs on the clean Ru(0001) terraces.

A way to produce more surface defects is by sputtering the surface with noble gas ions. The Ru(0001) surface was exposed to 100 nA 1 keV He^+ for 10 min followed by annealing to 700 K, and the result was that the sticking coefficient increased approximately by a factor of three.

In Fig. 8, a series of N_2 TPD spectra from the clean Ru(0001) surface are shown. They are in good agreement

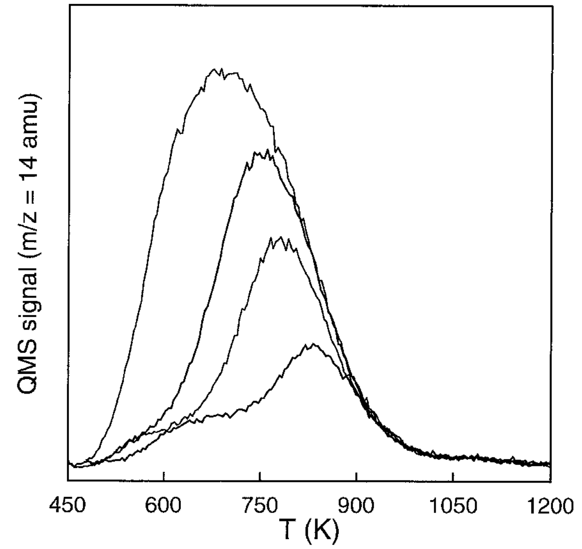

FIG. 8. N_2 TPD spectra ($m/z = 14$ amu) from clean Ru(0001). The heating rate was 4 K/s, and N_2 was adsorbed at 450 K. The N coverages are 0.25, 0.15, 0.10, and 0.06 ML.

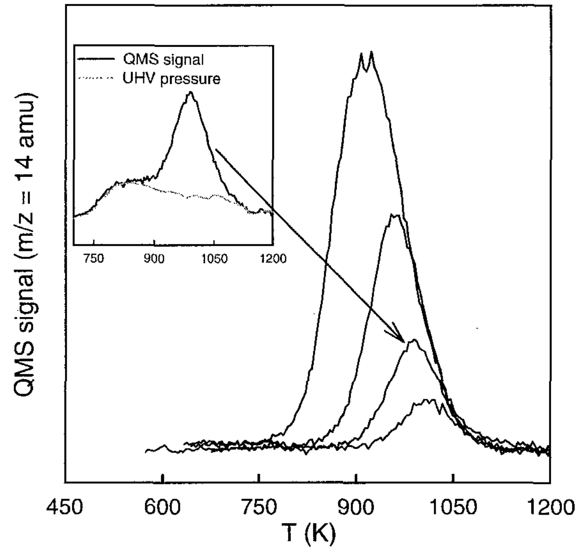

FIG. 9. N_2 TPD spectra ($m/z = 14$ amu) from Ru(0001) covered by approximately 0.05 ML of Au. The heating rate was 4 K/s, and N_2 was adsorbed at 700 K. The N coverages are 0.15, 0.07, 0.03, and 0.015 ML. A contribution to the TPD signal, originating from other surfaces, was subtracted according to the procedure described in the experimental section and is illustrated in the inset. Au will start to desorb from the surface at approximately 1200 K (27).

with spectra reported in the literature where the N coverage was established by other methods (12, 25, 26). Figure 9 displays similar TPD results for the Au-passivated Ru(0001) surface. In these spectra, "backgrounds" were subtracted as described earlier and are also illustrated in the inset.

By comparing Figs. 8 and 9, one sees that the addition of Au shifts the N_2 desorption peaks up in temperature by approximately 150 K, and there is a substantial narrowing of the peaks. Depositing Au after N_2 adsorption at 450 K resulted in TPD spectra similar to those in Fig. 9; i.e., the difference in desorption characteristics is not a result of the different temperatures used when nitrogen is adsorbed on the two surfaces.

4. DISCUSSION

N_2 Dissociation on the Clean Ru(0001) Surface

Based on our results an obvious conclusion would be that thermal N_2 dissociation on the clean Ru(0001) surface is totally dominated by step sites. However, from the experiments we cannot reject the possibility that highly active sites, other than steps, are responsible for the dissociation. Such sites could also be blocked by Au. Further evidence that step sites are the active sites is given by density-functional calculations (19), where the calculated dissociation barrier is about 35 kJ/mol at step sites while it is about 185 kJ/mol at the Ru(0001) terrace sites. This activation barrier at the step sites is in very good agreement with our activation energy for the clean surface.

The proposal that small amounts of alkali metal are responsible for the measured activity on the clean Ru(0001) surface (5) is not favored by theory. From density-functional calculations it was found that alkali metals only lower the barrier for N_2 dissociation on the Ru(0001) terraces by 30 kJ/mol or less (28), which is insufficient to bring the experimentally observed barrier close to the theoretical one. The fact that mild sputtering of the surface enhances the sticking coefficient by a factor of three is also in agreement with steps being the active sites for dissociating N_2.

Therefore, we are convinced that step sites are the active sites in dissociative adsorption of N_2 on the clean Ru(0001) surface. From the experiments it is also seen that the step sites are at least nine orders of magnitude more efficient to dissociate N_2 at 500 K than the terrace sites. To our knowledge, such a huge difference in reactivity between steps and terraces has never been reported for any other "metal surface/gas" system. A similar difference of six orders of magnitude was observed between H_2 adsorption on steps and terraces of the Si(100) semiconductor surface (20).

N_2 Dissociation on the Au-Passivated Ru(0001) Surface

It is an open question whether our results on the Au-passivated Ru(0001) surface reflect the true N_2 dissociation rate over the Ru(0001) terraces. It is possible that the measured rate results from a very small equilibrium concentration of unblocked step sites in the presence of Au. The activation barrier for such an adsorption mechanism will approximately be the activation energy for N_2 dissociation at the step site, plus the binding energy of Au at the Ru step relative to the second-most stable Au site on the surface. The latter is the energy cost of creating a step site free of Au. The second most stable site for Au adsorption is probably at the edge of Au adsorbed at an Ru step, and the relevant binding energy difference will be closely related to the difference in the surface energy of Au and Ru. This difference is of the order of 1 eV/atom (29). This mechanism for N_2 dissociation is therefore consistent with the barrier measured on the Au-passivated Ru(0001) surface. Other sites with higher activity than the terrace sites cannot be ruled out either, and diffusion of N from the areas on the surface which is not sufficiently passivated by Au is also a possibility. The density-functional calculations favor mechanisms other than dissociation at the terrace since the calculated N_2 dissociation barrier of 185 kJ/mol at the terrace (19) is significantly higher than the experimental barrier of 125 kJ/mol obtained for the Au-passivated Ru(0001) surface. Omitting s_0 determined at 620 K resulted in an experimental activation barrier of 165 kJ/mol, in better agreement with the calculations. However, the preexponential factor of 0.3 is high and requires that the transition state complex be fully mobile on the surface. Whatever the mechanism for N_2 dissociation on the Au-passivated surface is, the result of the measurements is an upper limit for the sticking

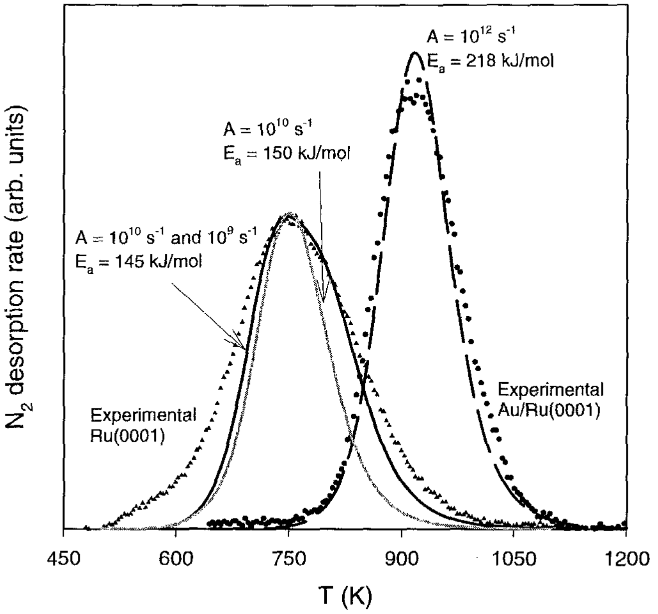

FIG. 10. Simulated N_2 TPD spectra assuming second-order desorption kinetics, a heating rate of 4 K/s, and an initial nitrogen coverage of 0.15 ML compared to similar experimental desorption spectra. The effective preexponential factors and the desorption barriers used are given in the figure. See text for discussion.

coefficient on the Ru(0001) terraces. Hence it can be concluded from the experiments alone that N_2 dissociation on the Ru(0001) terraces is, as the theoretical calculations suggest, a highly activated process.

N_2 Desorption from the Au-Passivated Ru(0001) Surface

The desorption curves from the Au-passivated surface fit well with second-order desorption kinetics using a desorption barrier of 218 kJ/mol and a preexponential factor of 1×10^{12} s^{-1} as seen in Fig. 10. The barrier of 218 kJ/mol is close to the result of density-functional calculations, where the barrier at the Ru(0001) terrace is about 230 kJ/mol (19). The desorption experiments suggest that Au is not leaving the steps below 900 K, where most of the nitrogen is still present on the Au-passivated surface but has desorbed from the clean surface. This supports the interpretation that the N_2 dissociation rates obtained at the Au-passivated Ru(0001) surface are the true rates at the Ru(0001) terraces since they were measured below 700 K.

N_2 Desorption from the Clean Ru(0001) Surface

The desorption of N_2 from the clean Ru(0001) surface occurs at lower temperature and has wider peaks compared to the Au-passivated Ru(0001) surface. The most plausible way to rationalize this shift in temperature is that nitrogen can diffuse to the steps on the clean Ru(0001) surface where desorption via a low barrier is possible, while this channel is blocked on the Au-passivated surface, forcing the desorption to take place over the high barrier at the Ru(0001) terrace.

Can desorption via steps explain both the broad desorption spectra and the shift in temperature? In an attempt to answer this question we have constructed a simple model for N_2 desorption from the clean Ru(0001) surface, where the desorption takes place at a step by second-order kinetics, and where the diffusion of N to the step is treated one-dimensionally. In the model the diffusion parameters measured by Zambelli *et al.* (23) are used. Guided by the density-functional calculations (19), a desorption barrier of 120 kJ/mol was chosen at the step. A preexponential factor of 1×10^{12} s^{-1} is assumed. One result of this model is that the diffusion is fast compared to desorption, and increasing the diffusion rate to infinity only results in a shift of the desorption peak by a few Kelvin; i.e., diffusion is not a limiting factor. The model also shows that desorption via the steps can be very well described as desorption from the whole surface with a lower effective preexponential factor. For example, if there is 1% of the step sites at the surface, the preexponential factor is reduced by a factor of 100. The simulated TPD peak temperature for an initial coverage of 0.15 ML of nitrogen is close to the experimental one if a desorption barrier of 150 kJ/mol is used together with an effective preexpontial factor of 1×10^{10} s^{-1}. The simulated spectrum is, however, too narrow, as seen in Fig. 10.

The step density is, of course, not homogeneous over the whole crystal surface; i.e., there are areas where the step density is different from the average density. As a consequence, the effective preexponential factor is not constant over the whole surface. This results in much broader TPD peaks, as seen in Fig. 10. Also shown here is the result of a simulation where the desorption barrier is 145 kJ/mol and the effective preexponential factor is 1×10^{10} s^{-1} for half the surface and 1×10^9 s^{-1} for the other half. Both the unknown step density distribution and the preexponential factor for desorption at the step will influence the shape of the spectrum, and therefore it is not relevant to do any fitting to obtain a precise desorption barrier. Nevertheless, the simulations show that N_2 desorption at the steps can explain the difference in nitrogen desorption between the clean Ru(0001) surface and the Au-passivated one. The desorption barrier of approximately 120 kJ/mol obtained from density-functional calculations (19) is not in significant disagreement with the 145 kJ/mol obtained from fitting the measurements.

All the dissociation and desorption barriers resulting from analyzing the experiments on nitrogen interaction with the Ru(0001) surface are summarized in Fig. 11. A sketch of the active site for N_2 dissociation at the Ru(0001) step is also shown in the figure. The geometry of this site is discussed below.

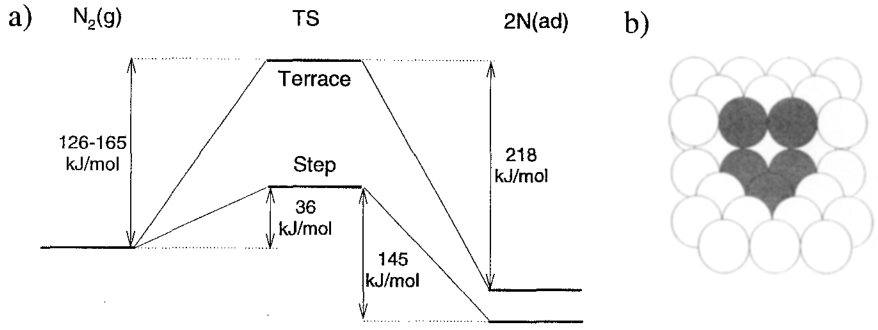

FIG. 11. (a) The dissociation and desorption barriers for nitrogen interacting with the Ru(0001) surface. The barriers were obtained from analyzing the experimental data presented here. TS is the transition state. (b) Sketch of the active site for N_2 dissociation (black atoms) at the Ru(0001) step as found by DFT calculations (19).

Comparison to Other Results on the N_2/Ru(0001) System

An important implication of the fact that thermal adsorption and desorption of N_2 on the clean Ru(0001) surface is dominated by the steps on the surface is that nearly all experiments that have been reported on N_2 adsorption and desorption on Ru(0001) have been measuring the activity of the step sites. Molecular beam experiments are exceptions that have mainly been probing the reactivity of the terrace sites. In support of this it has been shown in our laboratory that adding Au to the Ru(0001) surface only decreases the reactivity of the surface toward N_2 by a factor of two if the translational energy of the N_2 molecules is about 100 kJ/mol (19).

The higher reactivity of the step sites is explained by density-functional calculations as being the result of both an electronic effect and a geometrical effect (19). The lower coordination of the step atoms brings the d-band of these atoms closer to the Fermi level than the d-band of the terrace atoms, giving rise to a higher reactivity of the step atoms (30). The transition-state complexes at the step and at the terrace are quite similar; one nitrogen atom is sitting in a threefold hollow HCP site and one is sitting in a bridge site, the only exception is that no Ru atoms are nearest neighbors to both the N atoms at the step site, while this is the case for one Ru atom on the terrace. This strongly favors the step site since two N atoms bound to the same Ru atom give rise to a strong repulsive interaction (7). The picture is identical for NO dissociation at steps and terraces of the Ru(0001) surface, which has been investigated by Hammer using density-functional calculations (31). It is found that the geometrical effect is much more important than the electronic effect in stabilizing the transition state.

The geometry of the low barrier transition state is important when discussing the relationship between the reactivity of the clean Ru(0001) surface and the small Ru particles present in supported catalysts. From transmission electron microscopy (TEM) studies of Ru supported on MgO and SiO_2, it was reported that mainly the (0001), $(10\bar{1}0)$, and $(10\bar{1}1)$ faces are exposed at the surface of the Ru particles (32). Of these only the $(10\bar{1}0)$ has sites of five Ru atoms with a geometry where a threefold hollow HCP site and a bridge site are exposed close together. This also holds for some of the more open surfaces like the Ru$(11\bar{2}1)$ surface. Low-coordinated edge atoms will be part of some of these sites, and consequently there will be sites on the small crystals that have geometric and electronic properties similar to those of the step sites on the Ru(0001) surface. Hence, it is understandable that the barrier found in the present study of N_2 dissociation on the clean Ru(0001) surface is in good agreement with the barrier found on Ru catalysts (2, 3). The number of active sites will be a function of the number of edge sites and the total surface area of, e.g., the $(10\bar{1}0)$ facets. The relative number of edge sites increases when the Ru particles become smaller, and therefore small Ru particles are probably more efficient in dissociating N_2 than large particles, but only if the relative surface area of, for instance, the $(10\bar{1}0)$ facets is not decreasing too much. These arguments are not in conflict with the fact that the Ru$(10\bar{1}0)$ and the Ru$(11\bar{2}1)$ surfaces were not found to be significantly more reactive than the Ru(0001) surface in dissociating N_2 at room temperature (4), because even though the majority of the sites have the correct geometry they are not as low-coordinated, and are therefore not as active, as the step sites of the Ru(0001) surface.

That special step sites totally dominate N_2 dissociation on Ru would not have been the case if the adsorption energy of N at the steps had increased relative to the adsorption energy on the terrace by an amount equal to the decrease in transition state energy. In such a case the steps would very soon have been blocked by adsorbed N. For the same reason the special step sites probably dominate in the ammonia synthesis over Ru, since they are more reactive than other sites in the rate-determining step of N_2 dissociation without being significantly more blocked by the surface species involved in ammonia synthesis. This is the basis for using the present results as input to a microkinetic model for ammonia synthesis over Ru, which is the topic of the paper following this one (33). It is shown here that the approach is successful and therefore supports the proposal that active sites similar to the step sites on the Ru(0001) surface are present on the surface of small Ru particles.

The huge difference in reactivity between steps and terraces found in this work on N_2 dissociation at Ru(0001) might also be relevant for other systems of dissociative adsorption on low-index metal surfaces. It is therefore important to take this possibility into account when interpreting the results. In our work we used a new method to test the importance of steps by depositing small amounts of Au on the Ru(0001) surface. This approach is currently being tested on other systems.

5. CONCLUSIONS

Relying on the fact that small amounts of Au block the steps on the Ru(0001) surface, we have shown that steps totally dominate over terraces in thermal dissociation and desorption of N_2 over this surface. The steps sites are at least nine orders of magnitude more active in dissociating N_2 than the terrace sites. The initial sticking coefficient, s_0, was found to be $10^{-5.4\pm0.7} \times \exp(-36 \pm 5\,\mathrm{kJ\,mol^{-1}\,R^{-1}\,T^{-1}})$ on the clean surface and between $10^{-3.5\pm1.7} \times \exp(-126 \pm 21\,\mathrm{kJ\ mol^{-1}\ R^{-1}\ T^{-1}})$ and $10^{-0.5\pm2.7} \times \exp(-165 \pm 34\,\mathrm{kJ\ mol^{-1}\,R^{-1}\,T^{-1}})$ on the surface where the steps were blocked by 0.01–0.02 ML of Au. N_2 desorption from the clean Ru(0001) surface is also dominated by desorption from the steps. Simulations showed that the step density influenced the effective preexponential factor for desorption and that a desorption barrier of 145 kJ/mol is in good agreement with the N_2 TPD spectra from the clean Ru(0001) surface if a certain distribution of step density is taken into account. For N_2 desorption from the Au-passivated surface a barrier of 218 kJ/mol was found to fit the experiments. All the results are in good agreement with density-functional calculations as well as with earlier experimental observations on this system. However, several of these experiments should be reinterpreted so that the effect of steps are taken into account. We have argued that the step sites also will dominate in ammonia synthesis over Ru, and based on the knowledge of the low barrier transition state complex we find that similar sites are probably present on the small Ru particles in supported catalysts. This is the basis for the microkinetic model for ammonia synthesis over Ru presented in the following paper (33).

ACKNOWLEDGMENTS

Discussions and suggestions from J. K. Nørskov, B. Hammer, A. Logadottir, R. C. Egeberg, J. Sehested, and C. J. H. Jacobsen are gratefully acknowledged. The present work was in part financed by The Danish Research Councils through grant 9501775. The Center for Atomic-Scale Materials Physics (CAMP) is sponsored by the Danish National Research Foundation.

REFERENCES

1. Aika, K.-I., and Tamaru, K., *in* "Ammonia: Catalysis and Manufacture" (A. Nielsen, Ed.), p. 103. Springer–Verlag, Berlin/New York, 1995.
2. Rosowski, F., Hinrichsen, O., Muhler, M., and Ertl, G., *Catal. Lett.* **36**, 229 (1996).
3. Hinrichsen, O., Rosowski, F., Hornung, A., Muhler, M., and Ertl, G., *J. Catal.* **165**, 33 (1997).
4. Dietrich, H., Geng, P., Jacobi, K., and Ertl, G., *J. Chem. Phys.* **104**, 375 (1996).
5. Jacobi, K., Dietrich, H., and Ertl, G., *Appl. Surf. Sci.* **121/122**, 558 (1997).
6. Murphy, M. J., Skelly, J. F., Hodgson, A., and Hammer, B., *J. Chem. Phys.* **110**, 6954 (1999).
7. Mortensen, J. J., Morikawa, Y., Hammer, B., and Nørskov, J. K., *J. Catal.* **169**, 85 (1997).
8. Romm, L., Katz, G., Kosloff, R., and Asscher, M., *J. Phys. Chem. B* **101**, 2213 (1997).
9. Dahl, S., Taylor, P. A., Törnqvist, E., and Chorkendorff, I., *J. Catal.* **178**, 679 (1998).
10. Rosowski, F., Hornung, A., Hinrichsen, O., Herein, D., Muhler, M., and Ertl, G., *Appl. Catal. A* **151**, 443 (1997).
11. Stoltze, P., and Nørskov, J. K., *Phys. Rev. Lett.* **55**, 2502 (1985).
12. Shi, H., Jacobi, K., and Ertl, G., *J. Chem. Phys.* **99**, 9248 (1993).
13. Tsai, W., and Weinberg, H., *J. Chem. Phys.* **91**, 5302 (1987).
14. Taylor, H. S., *Proc. R. Soc. London Ser. A* **108**, 105 (1925).
15. Lang, B., Joyner, R. W., and Somorjai, G. A., *Surf. Sci.* **30**, 454 (1972); Davis, S. M., and Somorjai, G. A., *in* "The Chemical Physics of Solid Surfaces and Heterogeneous Catalysis" (D. A. King and D. P. Woodruff, Eds.), p. 217. Elsevier, Amsterdam/New York, 1982.
16. Ramsier, R. D., Gao, Q., Neergaard Waltenburg, H., and Yates, J. T., Jr., *J. Chem. Phys.* **251/252**, 6837 (1994).
17. Shincho, E., Egawa, C., Naito, S., and Tamaru, K., *Surf. Sci.* **149**, 1 (1985).
18. Zambelli, T., Wintterlin, J., Trost, J., and Ertl, G., *Science* **273**, 1688 (1996).
19. Dahl, S., Logadottir, A., Egeberg, R. C., Larsen, J. H., Chorkendorff, I., Törnqvist, E., and Nørskov, J. K., *Phys. Rev. Lett.* **83**, 1814 (1999).
20. Kratzer, P., Pehlke, E., Scheffler, M., Raschke, M. B., and Höfer, U., *Phys. Rev. Lett.* **81**, 5596 (1998).
21. Pötschke, G., Schröder, J., Günther, C., Hwang, R. Q., and Behm, R. J., *Surf. Sci.* **251/252**, 592 (1991); Hwang, R. Q., Schröder, J., Günther, C., and Behm, R. J., *Phys. Rev. Lett.* **67**, 3279 (1991).
22. Rasmussen, P. B., Holmblad, P. M., Christoffersen, H., and Chorkendorff, I., *Surf. Sci.* **287/288**, 79 (1993).
23. Zambelli, T., Trost, J., Wintterlin, J., and Ertl, G., *Phys. Rev. Lett.* **76**, 795 (1996).
24. Huang, H. H., Seet, C. S., and Xu, G. Q., *Surf. Sci.* **317**, 353 (1994).
25. Dietrich, H., Jacobi, K., and Ertl, G., *J. Chem. Phys.* **105**, 8944 (1996).
26. Hagedorn, C. J., Weiss, M. J., and Weinberg, H., *J. Vac. Sci. Technol. A* **16**, 984 (1998).
27. Niemantsverdriet, J. W., Dolle, P., Markert, K., and Wandelt, K., *J. Vac. Sci. Technol. A* **5**, 875 (1987).
28. Mortensen, J. J., Hammer, B., and Nørskov, J. K., *Phys. Rev. Lett.* **80**, 4333 (1998); Mortensen, J. J., Hammer, B., and Nørskov, J. K., *Surf. Sci.* **414**, 315 (1998).
29. Vitos, L., Ruban, A. V., Skriver, H. L., and Kollár, J., *Surf. Sci.* **411**, 186 (1998).
30. Hammer, B., Nielsen, O. H., and Nørskov, J. K., *Catal. Lett.* **46**, 31 (1997); Hammer, B., and Nørskov, J. K., *Surf. Sci.* **343**, 211 (1995).
31. Hammer, B., *Phys. Rev. Lett.*, in press.
32. Datye, A. K., Logan, A. D., and Lang, N. J., *J. Catal.* **109**, 76 (1988).
33. Dahl, S., Sehested, J., Jacobsen, C. J. H., Törnqvist, E., and Chorkendorff, I., *J. Catal.* **192**, 391 (2000).